Antarctic Science 34(5), 389–400 (2022) © The Author(s), 2022. Published by Cambridge University Press on behalf of Antarctic Science Ltd
doi:10.1017/S0954102022000335

Low-temperature investigation of residual water bound in free-living Antarctic *Prasiola crispa*

MAGDALENA BACIOR[1], HUBERT HARAŃCZYK[2], PIOTR NOWAK[3], PAULINA KIJAK[2], MONIKA MARZEC[2], JAKUB FITAS[4] and MARIA OLECH[5,6]

[1]*Department of Soil Science and Agrophysics, University of Agriculture in Kraków, Al. Mickiewicza 21, 31-120 Kraków, Poland*
[2]*Institute of Physics, Jagiellonian University, ul. Prof. Stanisława Łojasiewicza 11, 30-348 Kraków, Poland*
[3]*Faculty of Computer Science, Electronics and Telecommunications, AGH University of Science and Technology, Al. Mickiewicza 30, 30-059 Kraków, Poland*
[4]*Department of Mechanical Engineering and Agrophysics, University of Agriculture in Kraków, Al. Mickiewicza 21, 31-120 Kraków, Poland*
[5]*Institute of Botany, Jagiellonian University, ul. Kopernika 27, 31-501 Kraków, Poland*
[6]*Institute of Biochemistry and Biophysics, Polish Academy of Sciences, ul. Pawińskiego 5a, 02-106 Warsaw, Poland*
magdalena.bacior@urk.edu.pl

Abstract: Antarctic algae are extremophilic organisms capable of surviving harsh environmental conditions such as low temperatures and deep dehydration. Although these algae have various adaptations for life in extreme environments, the majority of the molecular mechanisms behind their resistance to dehydration and freezing are not yet fully understood. The aim of our research was to observe the behaviour of bound water freezing in the free-living Antarctic alga *Prasiola crispa*. One way to avoid frost damage involves deep dehydration of the algal thallus. For that reason, a detailed analysis of water freezing at different sample hydration levels was carried out. Nuclear magnetic resonance investigation revealed two types of water immobilization: cooperative bound water freezing for samples with sample hydration levels above $\Delta m/m_0 = 0.40$ and non-cooperative bound water immobilization for lower thallus hydration levels. In the differential scanning calorimetry experiment, 2-h incubation at -20°C suggested the diffusion and final binding of supercooled water to the ice nuclei and a lower hydration level threshold, at which ice formation could be observed ($\Delta m/m_0 = 0.21$). Our research provides a new perspective on water sorption and freezing in Antarctic algae, which may be important not only in biological systems, but also in such novel materials as metal-organic frameworks or covalent organic frameworks.

Received 5 August 2021, accepted 7 August 2022

Key words: alga, drought resistance, DSC, freezing resistance, NMR, phase growth

Introduction

Antarctic terrestrial algae are extremophilic organisms capable of surviving in harsh environmental conditions (Hájek *et al.* 2012, 2016, Gray *et al.* 2021). One way to withstand extremely low temperatures is via deep dehydration of the algal thallus; however, the molecular mechanisms of cold and drought resistance are not yet fully understood. Low temperature stresses biological systems as it reduces molecular motions and consequently affects the chemical and physical processes that take place in living organism. The effects of low-temperature stresses relate to reduced membrane fluidity, changes in intracellular pH and loss of macromolecular integrity (Clarke *et al.* 2013). The formation of ice crystals during the freezing of bound water in biological systems causes several additional types of cell damage (Bojic *et al.* 2021), and the rate of cooling affects the form of ice crystals created. Low cooling rates result in extracellular ice crystals whereas rapid cooling rates result in intracellular crystallites (Chang & Zhao 2021). During ice nucleation, solutes are excluded from the growing ice crystal and the concentration of solutes in the remaining liquid increases.

The analysis of water adsorption in porous materials improves our understanding of the physical and chemical properties of molecules inside the porous polymers of such novel materials as metal-organic frameworks (MOFs) or covalent organic frameworks (COFs; Zhou *et al.* 2018, Gao *et al.* 2019, Wang *et al.* 2019, Zhang *et al.* 2019). Water adsorbed on the surface of porous materials may reveal different properties than it does in its bulk form. This may be due to the interactions of molecules with the solid material as well as the increased surface-to-volume ratio of materials with smaller pores (Valiullin & Furo 2002).

The aim of our research was to observe the behaviour of water present in the foliose green alga *Prasiola crispa*

(Lightfoot) Menegh. upon cooling of the thallus to -63°C. *Prasiola crispa* provides a unique opportunity for study, as it is widespread in its free-living as well as lichenized form in the same Antarctic microenvironments. The lichenized form of *P. crispa*, *Turgidosculum complicatulum* (= *Mastodia tesselata*), is created by association with *Guingardia prasiolae* (Huiskes *et al.* 1997, Kovačik & Pereira 2001, Kovačik *et al.* 2003); however, some authors consider *Prasiola borealis* to be a photobiont of *T. complicatulum* (Pérez-Ortega *et al.* 2010).

Prasiola crispa is found in abundance in ice-free areas of Antarctica, especially in the supralittoral zone. This macroscopic terrestrial green alga has been the subject of much research (Santarius 1992, Jackson & Seppelt 1995, 1997, Tatur *et al.* 1997, Kovačik & Pereira 2001, Lud *et al.* 2001b, Kovačik *et al.* 2003, Graham *et al.* 2009, Kosugi *et al.* 2010, Richter *et al.* 2017, Fernández-Marín *et al.* 2019). *Prasiola crispa* is often found in wetter habitats than *T. complicatulum*, especially near meltwater streams (Lud *et al.* 2001a). Under natural conditions, *P. crispa* occurs in different growth forms, including unicellularly as well as with much more developed filaments. It may also form a sheet-like thallus. In its lichenization, tetrads of algal cells form packages interwoven with fungal hyphae that attach them to the substrate (Lud *et al.* 2001a). *Prasiola crispa* can be found on wet soils near bird colonies (especially penguin rookeries) rich in guano in the Maritime Antarctic and Continental Antarctica, where it forms wide, green 'carpets' (Jackson & Seppelt 1995, Kovačik & Pereira 2001, Graham *et al.* 2009). During the summer, in favourable habitats rich in nutrients, the dry mass of this algal colony may double every 2 weeks (Kovačik & Pereira 2001). Its main type of reproduction is fragmentation of the thallus, which may adapt to terrestrial environments (Kovačik *et al.* 2003). *Prasiola crispa* plays an important role in the succession of vegetation on abandoned penguin rookeries in the Maritime Antarctic (Tatur *et al.* 1997). *Prasiola crispa* experiences high levels of solar radiation, especially during summer, which may inhibit photosynthetic photon flux densities; it also endures repeated freeze/thaw cycles during spring and autumn as well as extremely low temperatures in winter, which cause the thallus to freeze (Jackson & Seppelt 1995, 1997, Lud *et al.* 2001b, Kosugi *et al.* 2010, Hájek *et al.* 2012). Photosynthetic activity of the *P. crispa* thallus was detected at temperatures as low as -15°C, although most of the intracellular water was frozen (Becker 1982). *Prasiola crispa* investigations create a unique opportunity for photobiont investigations, bypassing the need to prepare lichen thalli (Determeyer-Wiedmann *et al.* 2019).

This paper concerns the water-freezing mechanisms in *P. crispa* thalli. These mechanisms are not fully understood in the context of the sample hydration level. For that reason, the behaviour of bound water freezing was investigated at different sample hydration levels. The study was conducted with proton nuclear magnetic resonance (^{1}H-NMR) spectroscopy, relaxometry and differential scanning calorimetry (DSC). NMR is a powerful technique for investigating porous matter on the length scale from molecules to cells (Valiullin & Furo 2002), whereas DSC yields the temperature of water freezing and monitors the diffusion of supercooled water molecules to crystallization centres during the freezing of the sample. Our study shows two types of water immobilization: non-cooperative, for sample hydration levels below $\Delta m/m_0 = 0.39$ (where Δm is the mass of water taken up from the gaseous phase - this is taken as the difference between the mass of the sample taken during the experiment and the dry mass of the sample, m_0), and cooperative (with the formation of ice crystallites) for higher sample hydration levels. The two types of immobilization of water molecules at a low temperature are discussed in relation to the diffusion process.

Materials and methods

Field site

Free-living *P. crispa* thalli were collected near the Arctowski Polish Antarctic Station (centred at 62°09'41"S, 58°28'10"W), King George Island, Southern Shetlands, Maritime Antarctic, in January 2002, during the 26th Polish Antarctic Expedition of the Polish Academy of Sciences, close to sites populated by *T. complicatulum*. The samples were collected in the crevices of coastal rocks. They were situated on a thin layer of soil. The alga is a free-living organism that has a sheet-like, flattened thallus. It was identified using morphological and anatomical characteristics. *Prasiola crispa* thalli revealed morphological diversity. Mature plants had irregular, crisped, monostromatic blades creating green carpets. Cells were quadrate or rectangular and were clustered in groups with one layer of thick cells. Pyrenoids were at the centre of the chloroplasts. The thallus was medium to dark brownish-green and 2–20 mm in diameter. It was locally vesicular or cupulate, partially expanding to flat sheets with rhizoids. The thallus was filamentous (consisting of one or many series of cells) or foliaceous. At the time of the sample collection, during the summer, the air temperature was > 0°C.

After collection, the samples were stored under herbarium conditions at 22°C. The experimental work was carried out under laboratory conditions at the home institution. The hydration level of the air-dry sample was equal to $\Delta m/m_0 = 0.066 \pm 0.012$. The dry mass of the samples was measured after 72 h of heating at 70°C. This procedure was performed after all temperature

https://doi.org/10.1017/S0954102022000335 Published online by Cambridge University Press

measurements to achieve the sample hydration levels used in the experimental design. In order to obtain the different sample hydration levels, they were kept in desiccators over the surface of different salt solutions (Bacior *et al.* 2017). The hydration of each sample was designated as $\Delta m/m_0$ ($\Delta m = m - m_0$, where m is the mass obtained in a given desiccator).

^{1}H-NMR experimental parameters

The ^{1}H-NMR free induction decay (FID) measurements were carried out using a high-power WNS HB-65 NMR relaxometer constructed by Waterloo NMR Spectrometers (Waterloo, ON, Canada). The resonance frequency was 30 MHz (at the main static magnetic field, $B_0 = 0.7$ T), the transmitter power was 400 W and the length of the π/2 pulse was 1.5 µs. The obtained data were averaged over 1000 accumulations with a repetition time of 2 s, and they were analysed using the *CracSpin* program (Węglarz & Harańczyk 2000). The temperature was varied from 24.7°C to -62.3°C and was stabilized in a gaseous nitrogen stream. A wide range of temperatures were used to determine the freezing mechanisms of water in the algae as well as their adaptation strategy to harsh the Antarctic conditions.

The ^{1}H-NMR spectra were recorded on a Bruker Avance III spectrometer (Bruker Biospin, Billerica, MA, USA) operating at a resonance frequency of 300 MHz (at $B_0 = 7.0$ T) with the transmitter power used equal to 400 W. The length of the π/2 pulse was 2.2 µs.

^{1}H-NMR FID measurements

^{1}H-NMR measures the signal from hydrogen nuclei, and the intensity of the signal is proportional to the number of hydrogen nuclei. Measurement of the ^{1}H-NMR FIDs is a commonly used way to observe the ^{1}H-NMR signal. The FIDs can be parameterized by T_2^*. Free water has a T_2^* of approximately several seconds and ice has a T_2^* of < 5 µs. When water turns to ice, its ^{1}H-NMR signal is not measurable by the spectrometers used in this study; therefore, water freezing in bulk water can be followed precisely using these ^{1}H-NMR measurements as a complete loss of signal from the ice protons.

Alternatively, the Fourier transform of the ^{1}H-NMR FIDs represents the ^{1}H-NMR spectrum characterized by spectral widths that are related to T_2^*. Bulk water has a narrow linewidth of a few hertz, ice has a very broad linewidth that cannot be measured with the equipment used in this work and bound water has an intermediate linewidth of a few kilohertz. In many biological systems, including lichen, non-aqueous protons in lichen have a T_2^* of 10–20 µs and linewidths of a few tens of kilohertz. Water interacting with non-aqueous molecules has a much shorter T_2^* and a broader linewidth than bulk water - this is a consequence of time-dependent bonding to hydrophilic sites in the biological system's microstructure. The ^{1}H-NMR FID and ^{1}H-NMR spectrum measurements acquired here are equivalent: either approach could have provided all of the results from these experiments.

Temperature dependence of the ^{1}H-NMR FIDs

^{1}H-NMR FIDs for *P. crispa* thalli hydrated to $\Delta m/m_0 = 0.078$, 0.259 and 1.71 (Fig. S1), recorded from 24.7°C down to -62.3°C, were fitted well by the superposition of Gaussian component S and exponentially relaxing component L (Eq. (1)):

$$FID(t) = S \cdot \exp\left(-\left(\frac{t}{T_{2S}^*}\right)^2\right) + L_1 \cdot exp\left(-\frac{t}{T_{2L}^*}\right), \quad (1)$$

where T_{2S}^* is the proton spin-spin relaxation time for the solid component S, taken as the time required for the Gaussian function to decay to 1/e of its initial amplitude, whereas T_{2L}^* is the proton relaxation time of mobile protons of liquid component L (Harańczyk *et al.* 2006, 2012). The spin-spin relaxation times were shortened by B_0 inhomogeneities and their effective values were measured (Chavhan *et al.* 2009). The liquid signal expressed in the units of the solid signal (L/S) allowed for comparison of the data detected for dry and hydrated samples.

The data shown in Figs 1 & 2 were obtained from FID measurements carried out for selected samples with hydration levels of 0.078 and 1.71, respectively. For each sample hydration, FID signals were collected at 10 different temperatures: 24.7°C, 17.2°C, 7.5°C, -3.1°C, -13.1°C, -23.3°C, -32.8°C, -43.1°C, -52.9°C and -62.3°C.

In micro-heterogenous biological systems, separated spin subsystems have different relaxation times. Separated groups of spins form a solid matrix of the system, while other mobile molecular groups form tightly and loosely bound water pools. The total ^{1}H-NMR amplitude signal was normalized to 1 as a superposition of the signal S from the solid-state protons and of the signal L coming from the mobile protons of bound water fraction. The S or L signals do not give any useful information separately, but the liquid signal expressed in the units of the solid signal allows us to compare the data for dry and hydrated samples. The mobile component of the algal samples arises not only from bound water, but also from non-aqueous liquid components, as neutral lipids.

Temperature dependence of the ^{1}H-NMR spectra

The ^{1}H-NMR spectrum (Eq. (2)) may be successfully fitted by the superposition of the Gaussian line

https://doi.org/10.1017/S0954102022000335 Published online by Cambridge University Press

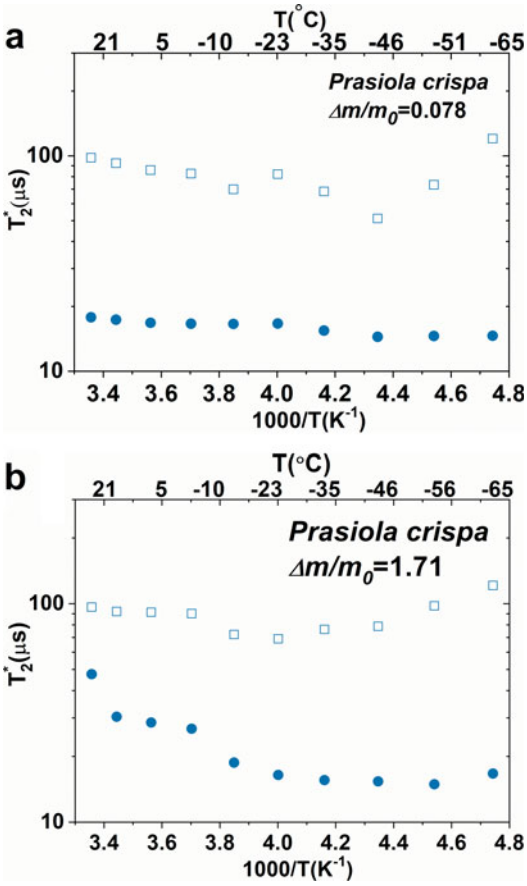

Fig. 1. a. Proton nuclear magnetic resonance (^{1}H-NMR) free induction decay (FID) times taken as a function of temperature for *Prasiola crispa* thalli hydrated to $\Delta m/m_0 = 0.078$. Solid Gaussian component (S) = closed circles, bound water fraction (L) = open squares. **b.** ^{1}H-NMR FID times taken as a function of temperature for *P. crispa* thalli hydrated to $\Delta m/m_0 = 1.71$. Solid Gaussian component (S) = closed circles, bound water fraction (L) = open squares.

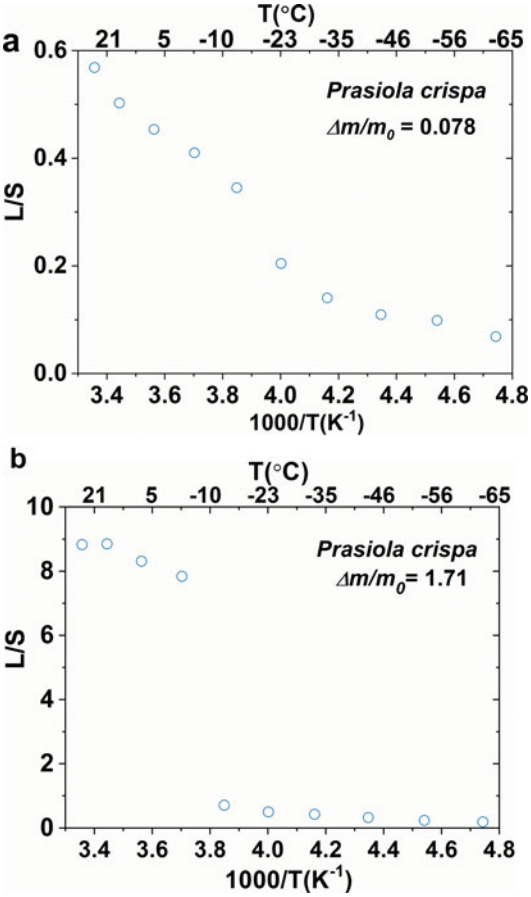

Fig. 2. Temperature dependence of the liquid signal amplitude, L/S, expressed in units of solid signal, recorded for *Prasiola crispa* thalli hydrated to **a.** $\Delta m/m_0 = 0.078$ and to **b.** $\Delta m/m_0 = 1.71$.

component with the area under the line equal to A_G, coming from significantly immobilized protons bound to the solid matrix, and one narrow Lorentzian line component with the area under the line equal to A_L, coming from mobile protons of the sample (from water bound in the algal thallus):

$$A(\nu) = y_0 + \frac{A_G}{\sqrt{\pi \ln 2}\Delta\nu_G}\exp\left[-2\cdot\left(\frac{\nu-\nu_G}{\sqrt{2\ln 2}\Delta\nu_G}\right)^2\right] + \frac{2A_L}{\pi}\left[\frac{\Delta\nu_L}{4(\nu-\nu_L)^2+(\Delta\nu_L)^2}\right], \quad (2)$$

where ν_G and ν_L are Gaussian and Lorentzian peak positions, respectively, while $\Delta\nu_G$ and $\Delta\nu_L$ are the line half-widths for the Gaussian and Lorentzian components of the ^{1}H-NMR line and y_0 is the constant signal component. The amplitude A is a dependent variable as a function of the magnetic field frequency (independent variable). For the *P. crispa* thalli hydrated to $\Delta m/m_0 = 0.08$, 0.311 and 0.486, the ^{1}H-NMR spectra were recorded at temperatures ranging from 23.8°C down to -61.3°C.

Differential scanning calorimetry

DSC measurements were taken using a PerkinElmer (Waltham, MA, USA) DSC 8000 calorimeter with 30 µL aluminium pans. The calibration of the calorimeter was performed using the melting points of indium and of water. The sample mass was ~8 mg. The temperature measurements were recorded from room temperature down to -60°C, then the samples were heated back to room temperature. These steps were conducted to detect the freezing/melting temperature of the water present in the sample. The rate of heating or cooling was equal to 2°C min^{-1}.

https://doi.org/10.1017/S0954102022000335 Published online by Cambridge University Press

DSC incubation experiment

During the incubation experiment, the sample was cooled down to -60°C, then heated up to -20°C, and after 2 h of incubation at this temperature it was warmed up to room temperature. A 2 h incubation of the sample at -20°C increases the mobility of water molecules in the sample; it is thus possible to observe the growth of ice crystallites, as water molecules migrate to the centres of crystallization. *Pyris* software (PerkinElmer, Waltham, MA, USA) was used to calculate the onset and peak temperatures as well as the transition enthalpies. A relatively long incubation time allowed water molecules to diffuse and to attach to presumably already-existing ice microcrystallites beyond the resolution of the calorimeter.

Statistical analysis

The one-dimensional procedure of the *CracSpin* program (Węglarz & Harańczyk 2000) was used to fit the ^{1}H-NMR FID signal (in time domain), where the solid component S is a Gaussian function and the liquid component L is an exponential function. The accuracy of the function was confirmed by the residual function, calculated as the difference between the fitted and the recorded values of the FID signal, which did not exceed a few percentage points for any recorded point (Fig. S1b).

The ^{1}H-NMR data were elaborated using *OriginPro* version 9.1 (OriginLab Corp., Northampton, MA, USA). This program allows for the arbitrary adjustment of the results as set by the user functions using the iterative Lavenberg-Marquardt algorithm. The R^2 value obtained for the entire dataset was ~0.99.

Results

Temperature dependence of the ^{1}H-NMR FIDs

Figures 1a & b show the temperature dependences of the proton spin-spin relaxation times T_2^* for the ^{1}H-NMR FID signal components recorded for *P. crispa* samples hydrated to $\Delta m/m_0 = 0.078$ and 1.71, respectively. The average values of the spin-spin relaxation times were equal to $T_{2L}^* \approx 82$ µs, 63 µs and 89 µs for the hydration levels of the sample equal to $\Delta m/m_0 = 0.078$, 0.259 and 1.71.

The temperature dependences of the total liquid signal expressed in units of the solid signal L/S are shown in Figs 2a & b & S3. The values shown in Fig. 2 were calculated from the FID measurements (Fig. S1) performed for the samples with different hydration levels ($\Delta m/m_0 = 0.078$, 0.259 and 2.429) and recorded from room temperature down to -63°C.

The typical FID signal is shown in Fig. S1. As temperatures decreased, the water molecules gradually became immobilized. In thalli of Antarctic lichen, where the fractions of tightly and loosely bound water were observed, a transition of the loosely bound (freezing) water pool to the tightly bound (non-freezing) water pool was observed, representing an adaptive mechanism to Antarctic conditions.

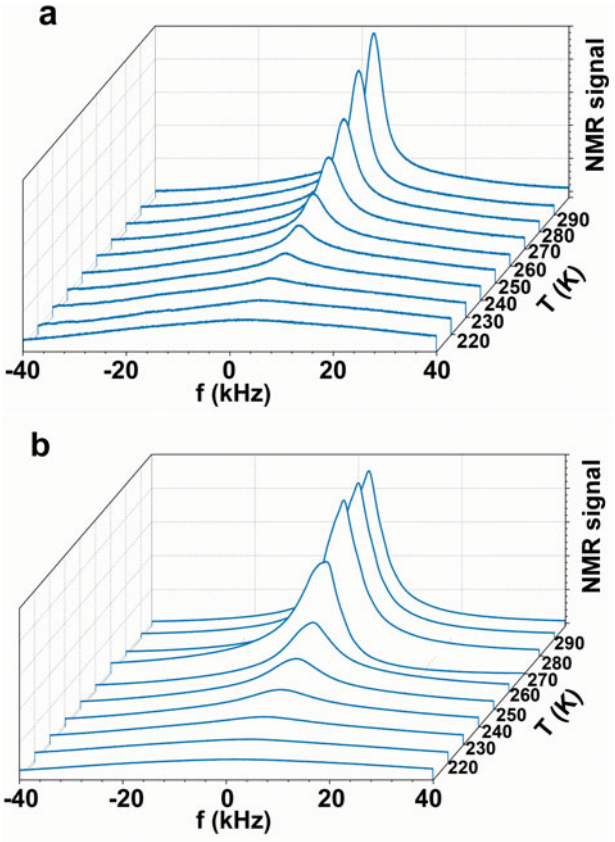

Fig. 3. a. Stacked plots of the proton nuclear magnetic resonance (^{1}H-NMR) spectra recorded as a function of temperature for *Prasiola crispa* thalli hydrated to $\Delta m/m_0 = 0.08$. **b.** Stacked plots of the ^{1}H-NMR spectra recorded as a function of temperature for *P. crispa* thalli hydrated to $\Delta m/m_0 = 0.486$.

The amplitude of the liquid signal decreased continuously with decreasing temperature for the samples of *P. crispa* thalli hydrated to $\Delta m/m_0 = 0.078$ and 0.259, which suggests non-cooperative bound water immobilization (Figs 2a & S3). Water freezing was detected for the sample hydrated to $\Delta m/m_0 = 1.71$ (Fig. 2b). The amplitude of the liquid-to-solid signal continuously decreased from room temperature down to -3.1°C, then a non-continuous gap was observed down to -13.1°C, suggesting water freezing in the sample.

Temperature dependence of the ^{1}H-NMR spectra

The ^{1}H-NMR spectrum (Fig. 3) was successfully fitted by the superposition of Gaussian component A_S coming from significantly immobilized protons of the sample

https://doi.org/10.1017/S0954102022000335 Published online by Cambridge University Press

and one narrow Lorentzian line component A_L coming from the mobile protons of the sample (Eq. S2).

When the temperature decreased down to -61.3°C, the half-widths of a broad line component increased, reaching the average values $\Delta\nu_G \approx 48.77$, 45.75 and 52.63 kHz for the samples hydrated to $\Delta m/m_0 = 0.08$, 0.311 and 0.486, respectively. This continuous increase suggests the gradual immobilization of protons during the cooling of the sample (Fig. 3). The more pronounced increase in half-widths of the Lorentzian function $\Delta\nu_L$ during the cooling of the sample suggests a reduced mobility of the supercooled water molecules.

Table I presents the parameters of the ^{1}H-NMR spectra recorded for *P. crispa* thalli at $t = 25$°C and -3°C at different hydration levels of the samples. At room temperature, the half-width of the solid Gaussian line component had $\Delta\nu_G$ values of 37.6–39.6 kHz (i.e. the Gaussian component width changes little with moisture content). The half-width of the mobile Lorentzian line component $\Delta\nu_L$ varied from 2.85 to 7.65 kHz for the hydration levels of $\Delta m/m_0 = 0.08$–0.486.

At different levels of thallus hydration for $\Delta m/m_0 = 0.08$–0.486 at -3°C, the half-width of the solid Gaussian line component decreased from $\Delta\nu_G = 46.1$ to 29.3 kHz (i.e. at -3°C, the solid component changed mobility as the moisture content increased). For the liquid component, the half-widths of the line for the mobile component $\Delta\nu_L$ were in the range of 3.25–7.88 kHz. The spin-spin relaxation time for the Gaussian line component was calculated from Eq. (3):

$$T_{2S}^{*} = \frac{\sqrt{2}}{\pi\Delta\nu G} \tag{3}$$

whereas for the mobile protons T_{2L}^{*} the spin-spin relaxation time was taken from Eq. (4):

$$T_{2L}^{*} = \frac{\sqrt{2}}{\pi\Delta\nu L}. \tag{4}$$

The temperature dependence of the total mobile proton signal (area under the line) expressed in units of the solid signal A_L/A_G is presented in Fig. 4. As observed in the time domain ^{1}H-NMR experiments, *P. crispa* thalli hydrated in the range of $\Delta m/m_0 = 0.08$–0.311 showed a continuous decrease in the liquid signal, coming from mobile protons with decreasing temperature (Figs 4a & S5). For the sample hydrated to $\Delta m/m_0 = 0.486$, cooperative immobilization of water was observed (Fig. 4b).

Table I. Proton nuclear magnetic resonance spectral parameters evaluated for *Prasiola crispa* thalli for the temperatures of 25°C down to -3°C at different sample hydration levels.

t (°C)	$\Delta m/m_0$	$\Delta\nu_G$ (kHz)	$\Delta\nu_L$ (kHz)	A_L/A_G
25	0.08	39.646 ± 0.088	3.990 ± 0.088	1.14 ± 0.25
-3	0.08	46.120 ± 0.056	5.567 ± 0.009	0.49 ± 0.06
25	0.311	37.580 ± 0.42	2.849 ± 0.004	4.36 ± 0.06
-3	0.311	38.990 ± 0.15	3.252 ± 0.004	2.13 ± 0.20
25	0.486	38.950 ± 0.32	7.647 ± 0.012	5.86 ± 0.07
-3	0.486	29.280 ± 0.33	7.881 ± 0.081	1.72 ± 0.07

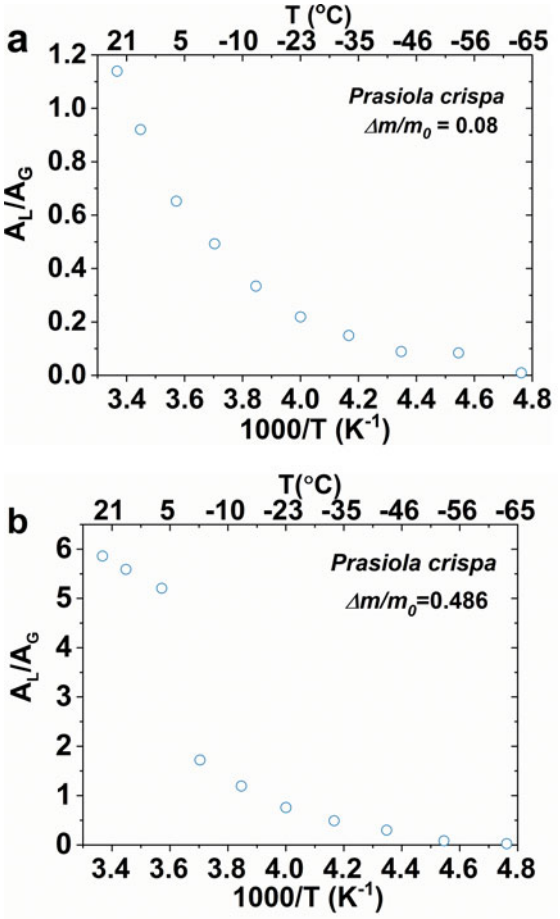

Fig. 4. a. The A_L/A_G temperature dependence for *Prasiola crispa* thalli hydrated to $\Delta m/m_0 = 0.08$. **b.** The A_L/A_G temperature dependence for *P. crispa* thalli hydrated to $\Delta m/m_0 = 0.486$.

DSC temperature measurements

DSC was used to monitor the bound water freezing (melting) in the samples. These measurements involved cooling and heating scans at the same cooling/heating rate of 2°C min^{-1}. Measurements performed for the driest sample ($\Delta m/m_0 = 0.08$) did not reveal any peaks coming from water freezing or ice melting in the *P. crispa* thalli (Figs S5–S8). At a higher hydration level ($\Delta m/m_0 = 0.25$), only an ice-melting peak was recorded during the heating of the sample and there was no water-freezing peak detected during cooling of the sample. For yet higher hydration levels of the sample (from $\Delta m/m_0 = 0.55$), the presence of a phase transition

https://doi.org/10.1017/S0954102022000335 Published online by Cambridge University Press

was detected either for water freezing or for ice melting. A linear increase of the onset temperatures for water freezing, t_f (and for ice melting, t_m), as a function of sample hydration level was detected for *P. crispa* thalli (Fig. 5) according to Eq. (5) and Eq. (6):

$$t_f = 23.8\Delta m/m_0 - (35.6 \pm 2.2)^{\circ}\mathrm{C} \quad (5)$$

$$t_m = (23.7 \pm 6.7)\Delta m/m_0 - (33.0 \pm 5.2)^{\circ}\mathrm{C} \quad (6)$$

The linear form suggests that the freezing onset temperature is correlated with the size of the water compartment in a porous material that characterizes the heterogenous ice-nucleation process.

The transition enthalpies for melting ΔH_m and for freezing ΔH_f linearly increased with increasing hydration levels (Fig. 6a) according to Eq. (7) and Eq. (8):

$$\Delta H_{m.} = (85 \pm 13)\Delta m/m_0 - (26.9 \pm 8.7) \quad (7)$$

$$\Delta H_{f.} = 85\Delta m/m_0 - (36.1 \pm 4.4) \quad (8)$$

This dependence allows one to determine the threshold hydration level at which the cooperative bound water freezing (ice formation) appears. For *P. crispa* thalli, no melting was detected (melting enthalpy was equal to 0) for the hydration levels of the thalli a $\Delta m/m_0 \leq 0.32 \pm 0.15$, whereas no freezing was detected (freezing enthalpy was 0) for the hydration levels $\Delta m/m_0 \leq 0.42 \pm 0.12$ (Fig. 6a). The average value of the threshold hydration level was equal to $\Delta m/m_0 = 0.37$. Quantitative decomposition of the recorded peaks into a symmetric part coming from the main ice-melting peak and a low-temperature shoulder (surplus in the enthalpy) was performed. The proportions of the low-temperature shoulder in the DSC peaks (Fig. 6b) for the different sample hydration levels were calculated and used to separately fit the hydration dependence of the area under the main peak ΔH_{mMP} and the low-temperature 'shoulder' ΔH_{mSh} according to Eq. (9) and Eq. (10):

$$\Delta H_{mMP} = (59 \pm 7.4)\Delta m/m_0 - (20.3 \pm 5.3) \quad (9)$$

$$\Delta H_{mSh} = 59\Delta m/m_0\ (27.7 \pm 4.8) \quad (10)$$

The melting enthalpy increased for the main peak as well as for the low-temperature shoulder with a similar slope when the hydration level was increased up to $\Delta m/m_0 = 0.8$, suggesting that the mass of water in both

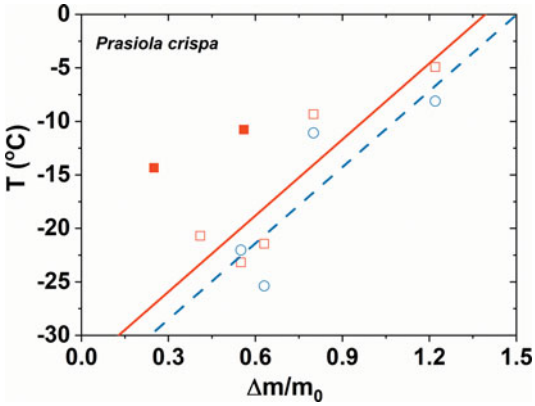

Fig. 5. The onset temperatures of ice melting (open squares) and water freezing (open circles) and of ice melting preceded by a 2 h incubation of the sample (closed squares) expressed as a function of the hydration level of *Prasiola crispa* thalli.

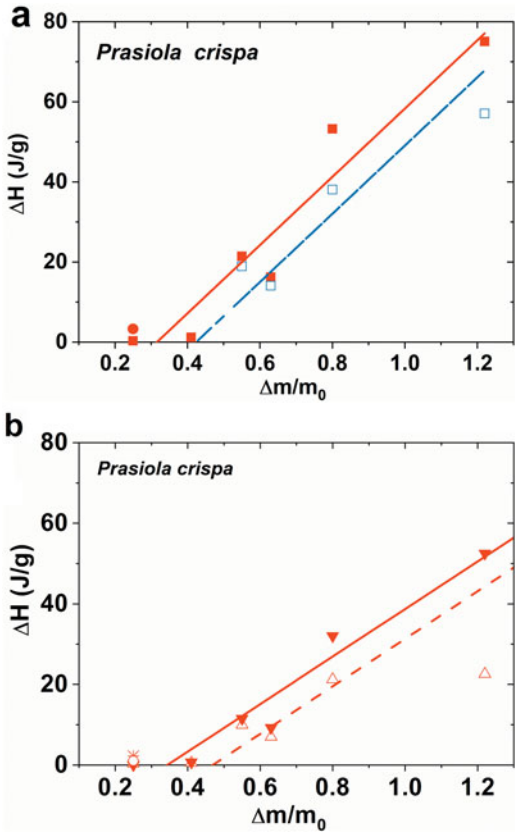

Fig. 6. a. Transition enthalpy ΔH expressed as a function of relative mass increase $\Delta m/m_0$ for bound water freezing (open squares) and ice melting (closed squares) and for ice melting after a 2 h incubation of the sample at -20°C (closed circles) observed for *Prasiola crispa* thalli. **b.** Transition enthalpy for ice melting after decomposition of differential scanning calorimetry peaks into two components: a mean melting peak (closed triangles) and a low-temperature 'shoulder' (open triangles), showing a main melting peak after a 2 h incubation of the sample at -20°C (star) and a low-temperature 'shoulder' after a 2 h incubation of the sample at -20°C (circle).

https://doi.org/10.1017/S0954102022000335 Published online by Cambridge University Press

subsystems increased similarly and did not saturate within the range of hydration levels investigated. For the *P. crispa* thalli hydrated to the highest level ($\Delta m/m_0 = 1.22$), the melting enthalpy related to the low-temperature shoulder (Fig. 6b) differed from that of the thalli of the lichen *T. complicatulum*.

DSC incubation experiment

The DSC incubation experiment was performed for *P. crispa* thalli hydrated to $\Delta m/m_0 = 0.25$ (no or only residual freezing/melting peak was expected). At the end of the incubation process, the sample was warmed up to room temperature. A pronounced melting peak was detected. The warming thermogram without the 2 h incubation is shown in Fig. 7a, while the warming thermogram after 2 h of incubation at -20°C is presented in Fig. 7b. The melting enthalpy determined without the incubation process was equal to $\Delta H = 0.34$ J g^{-1}, whereas after the incubation process this value was equal to $\Delta H = 3.30$ J g^{-1}.

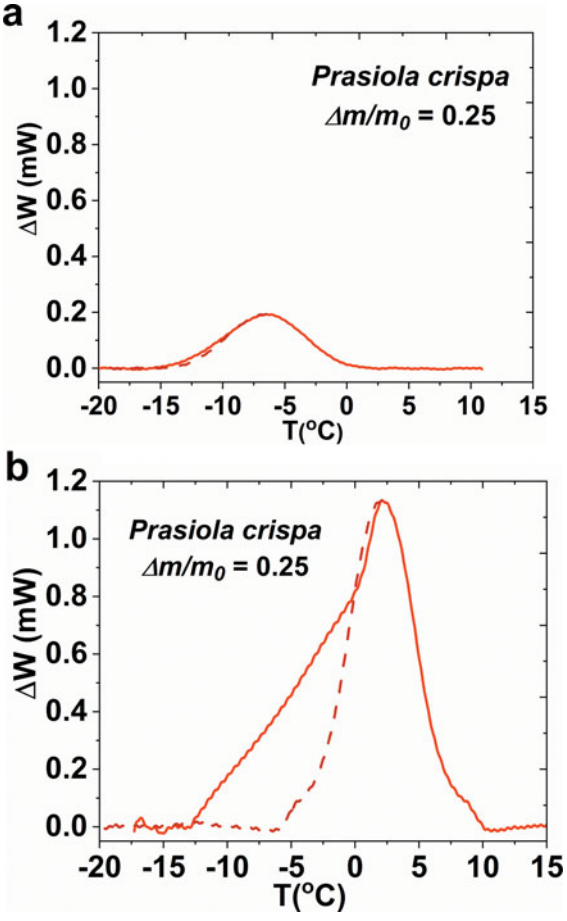

Fig. 7. a. Differential scanning calorimetry (DSC) heating termogram for *Prasiola crispa* thalli hydrated to $\Delta m/m_0 = 0.25$ and **b.** DSC heating termogram of the same sample but recorded after a 2 h incubation at -20°C. Each peak was decomposed into two components: a main peak (dashed line) and a low-temperature 'shoulder'. The heating rate was equal to 2°C min^{-1}.

Discussion

The relaxation of the spin subsystems with different values for the relaxation time was observed. A solid matrix of the organism was marked by significantly immobilized protons, while the mobile proton group constituted the tightly bound water pool. Single-component water relaxation was observed in *P. crispa* thalli, meaning that there was only one fraction of bound water in the sample (Fig. S1). The transverse spin-spin relaxation time T_2^* recorded by the ^{1}H-NMR was inversely proportional to the correlation time τ_c characterizing the rotational mobility of protons. When protons rotate quickly (as in the case of protons of the loosely bound water pool), the rotational correlation time τ_c is shorter and thus the relaxation time is longer. By contrast, water molecules situated in the proximity of the pore walls of the sample have longer correlation times (shorter T_2^*) as their rotation is hindered. This is particularly evident in Antarctic lichens, as well as in lyophilized photosynthetic membranes, where tightly and loosely bound water fractions differing in their T_2^* relaxation times were found (Harańczyk *et al.* 2012, 2016, 2021, Nowak *et al.* 2018). The decrease in temperature causes the gradual immobilization of water molecules, which form ice crystallites. The correlation time increases with decreasing relaxation time. The residual fraction of unfrozen water remains between the ice crystallites and the algal surface.

The ^{1}H-NMR FIDs were registered at different temperatures (from 25°C down to -63°C) and were fitted by a superposition of the solid component coming from immobilized protons of the algal thallus and one exponentially relaxing component coming from the tightly bound water fraction. In contrast, in the lichenized form of *P. crispa*, both tightly and loosely bound water fractions were detected (Bacior *et al.* 2019). The loosely bound water fraction was not detected even at high levels of sample hydration (i.e. there was no free water). These differences can be explained by the different structures between the alga and its lichenized form. Lichens are symbiotic organisms formed most often of a fungus and an alga; lichen thalli are formed differently from the thalli of *P. crispa*. Additionally, *P. crispa* as a photobiont of *T. complicatulum* appears in the lichen thalli in a coccal state (Lud *et al.* 2001a). The alga *Klebsormidium*, from King George Island, Antarctica, has a similar structure to *P. crispa*. It is made up of filaments with 500–1000 cells and grows in very compact tufts (Elster *et al.* 2008). The average value of the spin-spin relaxation time recorded for the solid signal component

https://doi.org/10.1017/S0954102022000335 Published online by Cambridge University Press

of *P. crispa* at different sample hydration levels (Figs 1 & S2) was equal to $T_{2S}^{*} \approx 19$ μs (corresponds to the second moment $M_2 \approx 3 \times 10^9$ s^{-2}), which is a value close to that obtained for lichens (e.g. for *T. complicatulum* thalli $T_{2S}^{*} \approx 18$ μs, for *Umbilicaria aprina* $T_{2S}^{*} \approx 19$ μs) and for other biological systems such as photosynthetic membranes or DNA and didecyldimethylammonium chloride ($C_{19}H_{42}CIN$) complexes (DNA-DDCA) (Harańczyk 2003, Harańczyk *et al.* 2009, 2012). The Gaussian component of the ^{1}H-NMR line gradually broadened as the temperature decreased (Fig. 3), which suggests increased immobilization of the protons building the algal thallus. The half-width of the Lorentzian line component also increased with decreasing temperature due to the gradual immobilization of water molecules.

Many experiments show that the temperature of heterogenous ice nucleation depends on the sizes of the water compartments in the biological systems (Angell 1982, Wilson *et al.* 1999, 2003, Inada *et al.* 2001, Heneghan & Haymet 2002, Heneghan *et al.* 2002). For larger volumes of water, it is more difficult to attain low-temperature nucleation because there is a greater probability of encountering ice nuclei, thus the initiation of the freezing process takes place at a higher temperature (Wilson *et al.* 2003). The experiment performed on 5 μL of bulk water revealed that it freezes in the temperature range from approximately -21°C to -25°C (Wilson *et al.* 1999), whereas large volumes of water equal to 200 μL freeze at -14°C (Harańczyk 2003).

The DSC measurements of *P. crispa* thalli revealed that the onset temperatures of water freezing and ice melting linearly increase with increased hydration level of the thalli. This process, promoted by ice-nucleation activators, is also characteristic of other biological systems, such as bacteria, fungi, insects, plants and lichens (Kawahara 2013). At lower thalli hydration, the freezing point of the water connected to the sample was lower and reached -25°C for the hydration level $\Delta m/m_0 = 0.6$ compared to the more hydrated samples ($\Delta m/m_0 = 1.2$) for which the freezing point equalled -8°C. A similar dependence on the onset temperatures was detected for *T. complicatulum* thalli as well as for other lichen genera (Harańczyk 2003, Harańczyk *et al.* 2012). The analysis of the onset temperatures for the ice melting and water freezing of *P. crispa* thalli (Fig. 5) demonstrated a higher value of the slope for the line fitted to the experimental data ($a_{P.f} \approx 24$, where $a_{P.f}$ means the slope for the line registered for the freezing of *P. crispa* samples) compared to the value determined for *T. complicatulum* thalli ($a_{T.f} \approx 19$, where $a_{T.f}$ means the slope for the line registered for the freezing of *T. complicatulum* samples; Bacior *et al.* 2019). It is already known that sugar, alcohol and other substances may lower the freezing point in lichens. For this reason, the thalli of *P. crispa* hydrated to higher levels may freeze at higher temperatures than those of *T. complicatulum* collected from the same habitat. These data are consistent with data obtained for the same samples at different hydration levels by Bacior *et al.* (2017, 2019), where the significant presence of water-soluble substances was observed in the thalli of *T. complicatulum*, as well as with results obtained by Fernández-Marin *et al.* (2019), where a higher freezing tolerance of *P. crispa* in its lichenized form was suggested. The DSC peaks recorded for *P. crispa* thalli were asymmetric in form and were decomposed into the main transition peak and the low-temperature 'shoulder'. This asymmetry significantly increased after 2 h of incubation at -20°C; however, there are some differences seen in the quantitative analyses performed for the free-living *P. crispa* and for its lichenized form (Bacior *et al.* 2019). In lichenized thalli of *P. crispa*, the proportion of the main peak compared to the low-temperature shoulder was $\Delta H_{mp}/\Delta H_s = 0.55$, whereas for *P. crispa* it was $\Delta H_{mp}/\Delta H_s = 2.1$. This difference may be related to the structural differences in these two forms of *P. crispa* thalli and suggests that in the lichenized form the frozen water molecules may be gradually thawing, leading to a greater contribution to the 'shoulder' part of the peak. The incubation experiment showed the diffusion of supercooled, separated water molecules to the ice nuclei. The DSC courses recorded after the 2 h incubation of *P. crispa* thalli at -20°C gave the threshold hydration level at which ice melting was detected as equal to $\Delta m/m_0 = 0.21$. This value was significantly higher than that for *T. complicatulum* thallus where the lowest hydration level for melting detection was equal to $\Delta m/m_0 = 0.084$ (Bacior *et al.* 2019). This difference may be related to other factors in addition to the higher number of crystallization centres in the thalli of the lichenized form of *P. crispa*. Comparing the low-temperature water immobilization observed in the DSC calorimetry courses in free-living *P. crispa* thalli and in its lichenized form (*T. complicatulum*) hydrated to $\Delta m/m_0 = 0.25$ and collected from the same habitat in Antarctica, a significant difference could be observed, in that the melting enthalpy measured for free-living *P. crispa* was lower than that of its lichenized form (Bacior *et al.* 2019) before ($\Delta H = 0.34$ J g^{-1} for *P. crispa* and $\Delta H = 1.5$ J g^{-1} for *T. complicatulum*) as well as after the 2 h incubation of the sample ($\Delta H = 3.3$ J g^{-1} for *P. crispa* and $\Delta H = 6.1$ J g^{-1} for *T. complicatulum*), which may indicate that a smaller amount of water forms ice crystallites (whereas a larger amount remains in the supercooled phase) in the pores of the lichenized form of *P. crispa* than in its free-living form. The DSC measurements indicate that greater energy is needed to create an ice crystallite in the lichenized form of *P. crispa* than in its free-living form, which also suggests that the free-living *P. crispa* has less freezing resistance. This may, in turn, indicate that lichenized cells are more resistant to freezing.

https://doi.org/10.1017/S0954102022000335 Published online by Cambridge University Press

In its natural habitat, *P. crispa* is adapted to wide temperature fluctuations. On the other hand, the increased amount of cryoprotectant in the algal thallus may protect it against frost damage during the growth of ice crystallites connected with the migration of water molecules to the centres of crystallization. A large increase in proline, which probably plays a role as a cryoprotectant in the *P. crispa* thallus, has been observed in early winter (up to 28.4 ± 2.9 μmol g^{-1} of dry mass in mid-April from 1.2 ± 0.1 μmol g^{-1} of dry mass in January), and this was connected with photosynthetic activity after melting (Jackson & Seppelt 1995). Amino acids and other solutes protect this photosynthetic activity during freezing (Santarius 1992). One of cryoprotective mechanisms often used by terrestrial organisms is extracellular ice formation. In this process, a water vapour pressure gradient is created between the inside and the outside parts of the cells, which leads to a further outflow of water from the interior parts of the cells. As a consequence, intracellular dehydration continues. This dehydration process may preserve the interior parts of the algal cells against freezing and protect against the growth of ice crystallites inside the cells. At the same time, it causes an increased concentration of solutes, which protects the thallus against frost (Benson *et al.* 2007). At freezing temperatures, in the presence of ice the existence of unfrozen water may be caused by the freezing-point depression due to the presence of small solutes, macromolecules, membranes and other hydrophilic ultrastructures or by the effect of viscosity (Wolfe *et al.* 2002). Many freeze-tolerant organisms accumulate multiple cryoprotectants, including antifreeze proteins, glycoproteins or glycolipids, which inhibit ice formation or ice-crystal growth (Storey & Storey 1996, Duman 2001).

It seems that in biological systems (such as lichens or algae) there is a sample hydration level above which the cooperative water freezing is observed (with a strong discontinuity in the temperature dependence of the liquid amplitude of the signal, L/S) and below which the non-cooperative immobilization of water is preferred (as in the case of dry samples). In free-living *P. crispa* thalli, a similar mechanism was observed. A few scenarios for this could be proposed based on our results: ^{1}H-NMR measurements showed the non-cooperative immobilization of water bound in *P. crispa* thalli for the hydration level of $\Delta m/m_0 \leq 0.40$. In this hydration range, the temperature dependence of the liquid-to-solid amplitude (L/S) has a gentler slope. For the samples with hydration levels of $\Delta m/m_0 \geq 0.40$, the temperature dependence of the liquid-to-solid amplitude (L/S) revealed a step decrease in the liquid signal, which is characteristic of water freezing. The transfer of the loosely to tightly bound water fraction characteristic of lichens (Harańczyk *et al.* 2012, Nowak *et al.* 2018) was absent here, suggesting another structure of the free-living form of the alga, with smaller pore sizes in which the water molecules could still rotate but with longer rotational correlation times and thus with shorter spin-spin relaxation times. Data analysis suggests that down to -63°C the co-existence of ice crystallites as well as a supercooled interfacial water fraction within the pores of *P. crispa* thalli is probable. The co-existence of a non-freezing water fraction was supported by the temperature dependencies of proton spin-spin relaxation times T_2^*, which did not change during the temperature drop ($T_2^* \approx 100$ μs), suggesting that the correlation times of the residual interfacial water remained unchanged during the water freezing in the pores. The DSC analysis yielded the water-freezing threshold value of the hydration level at which cooperative bound water freezing was detected at $\Delta m/m_0 = 0.37$, which was a similar value to that obtained by ^{1}H-NMR.

These investigations provide a new perspective on water adsorption in porous materials and its freezing, which may have some applications not only in biological systems but also in water recycling, catalysts and fossil fuel studies (Zhou *et al.* 2018, Gao *et al.* 2019, Wang *et al.* 2019, Zhang *et al.* 2019). By using ^{1}H-NMR relaxometry and spectrometry as well as DSC, it is possible to monitor water molecule motions in the interfacial layer during the cooling of samples.

Conclusions

This study sheds light on the molecular dynamics of water bound in the Antarctic alga *P. crispa*. We found that algae samples with different levels of hydration revealed different mechanisms of water freezing. Namely, for dry samples below the hydration level of 0.39, non-cooperative immobilization of water molecules prevails, while cooperative water freezing was observed above this value. As the temperature decreased, the gradual immobilization of water molecules was observed, leading to the formation of ice crystals.

The DSC measurements showed that the freezing point of the sample water decreased with increasing dehydration, indicating the presence of heterogenous nucleation. The enthalpy of melting determined for the free-living form of *P. crispa* was lower than that for the lichenized form of this alga, which may indicate that the free-living form is less resistant to freezing.

Only one fraction of bound water was found in *P. crispa*, in contrast to Antarctic lichens, in which two fractions of bound water are present. Analysis of the data suggests that up to -63°C a fraction of supercooled water was found in the sample in addition to ice crystallites.

There are still many unanswered questions regarding how Antarctic organisms, especially the alga *P. crispa*, cope with harsh Antarctic conditions such as low

https://doi.org/10.1017/S0954102022000335 Published online by Cambridge University Press

temperatures and deep dehydration. Combined DSC and ^{1}H-NMR techniques are powerful tools that can be used to improve our understanding of the molecular mechanisms of cold and drought resistance.

Acknowledgements

We would like to thank the reviewers for their comments and suggested improvements.

Financial support

The research was carried out with equipment purchased thanks to the financial support of the European Regional Development Fund in the framework of the Polish Innovation Economy Operational Program (contract no. POIG.02.01.00-12-023/08) and financed by the Polish Ministry of Science and Higher Education (MNiSW, contract no. 7150/E-338/M/2015 and 7150/E-338/M/2016).

Author contributions

MO conducted the sampling. MB performed the laboratory work and data analyses and wrote the manuscript with support and assistance from HH. PN, PK, MM and JF performed the laboratory work.

Supplementary material

Eight supplemental figures will be found at https://doi.org/10.1017/S0954102022000335.

References

Angell, C.A. 1982. Supercooled water. *In* Franks, F., *ed. Water and aqueous solutions at subzero temperatures*. Water: a comprehensive treatise, vol. 7. New York: Plenum Press, 1–81.

Bacior, M., Nowak, P., Harańczyk, H., Patryas, S., Kijak, P. & Ligęzowaska, A. 2017. Extreme dehydration observed in Antarctic *Turgidosculum complicatulum* and in *Prasiola crispa*. *Extremophiles*, **21**, 331–343.

Bacior, M., Harańczyk, H., Nowak, P., Kijak, P., Marzec, M., Fitas J. & Olech, M.A. 2019. Low-temperature immobilization of water in Antarctic *Turgidosculum complicatulum* and in *Prasiola crispa*. Part I. *Turgidosculum complicatulum*. *Colloid Surfaces B: Biointerfaces*, **173**, 869–875.

Becker, E.W. 1982. Physiological studies on Antarctic *Prasiola crispa* and *Nostoc commune* at low temperatures. *Polar Biology*, **1**, 99–104.

Benson, E., Harding, K. & Day, J.G. 2007. Algae at extremely low temperatures. *In* Seckbach, J., *ed.*, *Algae and cyanobacteria in extreme environments*. Berlin: Springer, 365–383.

Bojic, S., Murray, A., Bentley, B.L., Spindler, R., Pawlik, P., Cordeiro, J.L., *et al*. 2021. Winter is coming: the future of cryopreservation. *BMC Biology*, **19**, 56.

Chang, T. & Zhao, G. 2021. Ice inhibition for cryopreservation: materials, strategies and challenges. *Advanced Science*, **8**, 2002425.

Chavhan, G.B., Babyn, P.S., Thomas, B., Shroff, M.M. & Haacke, E.M. 2009. Principles, techniques, and applications of T_2*-based MR imaging and its special applications. *Radiographics*, **29**, 1433–1449.

Clarke, A., Morris, G.J., Fonesca, F., Murray, B.J. & Acton, E. 2013. A low temperature limit for life on Earth. *PLoS One*, **8**, e66207.

Determeyer-Wiedmann, N., Sadowsky, A., Convey, P. & Ott, S. 2019. Physiological life history strategies of photobionts of lichen species from Antarctic and moderate European habitats in response to stressful conditions. *Polar Biology*, **42**, 395–405.

Duman, J.G. 2001. Antifreeze and ice nucleator proteins in terrestrial arthropods. *Annual Review of Physiology*, **63**, 327–357.

Elster, J., Degma, P., Kováčik, L., Valentová, L., Šramowá, K. & Pereira, A.B. 2008. Freezing and desiccation injury resistance in the filamentous green alga *Klebsormidium* from the Antarctic, Arctic and Slovakia. *Biologia*, **63**, 843–851.

Fernández-Marín, B., López-Pozo, M., Perera-Castro, A.V., Arzac, M.I., Saenz-Cenceros, A., Colesie, C., *et al*. 2019. Symbiosis at its limits: ecophysiological consequences of lichenization to the genus *Prasiola* in Antarctica. *Annals of Botany*, **20**, 1–16.

Gao, Y., Zhang, Y., Yang, Y., Zang, J. & Gu, F. 2019. Molecular dynamics investigation of interfacial adhesion between oxidised bitumen and mineral surfaces, *Applied Surface Science*, **479**, 449–462.

Graham, L.E., Graham, J.M. & Wilcox, L.W. 2009. *Algae*, 2nd edition. San Francisco, CA: Pearson Benjamin Cummings, 616 pp.

Gray, A., Krolikowski, M., Fretwell, P., Convey, P., Peck, L.S., Mendelowa, M., *et al*. 2021. Remote sensing phenology of Antarctic green and red snow algae using worldview satellites. *Frontiers in Plant Science*, **12**, 671981.

Hájek, J., Barták, M., Hadrová, J. & Forbelská, M. 2016. Sensitivity of photosynthetic processes to freezing temperature in extremophilic lichens evaluated by linear cooling and chlorophyll fluorescence. *Cryobiology*, **73**, 329–334.

Hájek, J., Vaczi, P., Bartak, M. & Jahnova, L. 2012. Interspecific differences in cryoresistance of lichen symbiotic algae of genus *Trebouxia* assessed by cell viability and chlorophyll fluorescence. *Cryobiology*, **64**, 215–222.

Harańczyk, H. 2003. *On water in extremely dry biological systems*. Post-doctoral dissertation, Jagiellonian University, 276 pp.

Harańczyk, H., Leja, A. & Strzałka, K. 2006. The effect of water accessible paramagnetic ions on subcellular structures formed in developing wheat photosynthetic membranes as observed by NMR and by sorption isotherm. *Acta Physica Polonica A*, **109**, 389–398.

Harańczyk, H., Leja, A., Jemioła-Rzemińska, M. & Strzałka, K. 2009. Maturation processes of photosynthetic membranes observed by proton magnetic relaxation and sorption isotherm. *Acta Physica Polonica A*, **115**, 526–532.

Harańczyk, H., Nowak, P., Lisowska, M., Florek-Wojciechowska, M., Lahuta, L.B. & Olech M.A. 2016. A method of water-soluble solid fraction saturation concentration evaluation in dry thalli of Antarctic lichenized fungi, *in vivo*. *Biochemistry and Biophysics Reports*, **6**, 226–235.

Harańczyk, H., Nowak, P., Bacior, M., Lisowska, M., Marzec, M., Florek, M. & Olech, M.A. 2012. Bound water freezing in Antarctic *Umbilicaria aprina* from Schirmacher Oasis. *Antarctic Science*, **24**, 342–352.

Harańczyk, H., Strzałka, K., Kubat, K., Andrzejowska, A., Olech, M., Jakubiec, D., *et al*. 2021. A comparative analysis of gaseous phase hydration properties of two lichenized fungi: *Niebla tigrina* (Follman) Rundel & Bowler from Atacama Desert and *Umbilicaria antarctica* Frey & I. M. Lamb from Robert Island, Southern Shetlands Archipelago, Maritime Antarctica. *Extremophiles*, **25**, 267–283.

Heneghan, A.F. & Haymet, A.D.J. 2002. Liquid-to-crystal nucleation: improved lag-time apparatus to study supercooled liquids. *Journal of Chemical Physics*, **117**, 5319–5327.

Heneghan, A.F., Wilson, P.W. & Haymet, A.D. 2002. Statistics of heterogeneous nucleation of supercooled water, and the effect of an added catalyst. *Proceedings of the National Academy of Sciences of the United States of America*, **99**, 9631–9634.

Huiskes, A.H.L., Gremmen, N.J.M. & Francke, J.W. 1997. The delicate stability of lichen symbiosis: comparative studies on the photosynthesis of the lichen *Mastodia tessellate* and its free-living phycobiont, the alga *Prasiola crispa*. *In* Battaglia, B., Valencia, J. & Walton, D.W.H., *eds.*, *Antarctic communities: species, structure and survival*. Cambridge: Cambridge University Press, 234–240.

Inada, T., Zhang, X., Yabe, A. & Kozawa, Y. 2001. Active control of phase change from supercooled water to ice by ultrasonic vibration 1. Control of freezing temperature. *International Journal of Heat and Mass Transfer*, **44**, 4523–4531.

Jackson, A.E. & Seppelt, R.D. 1995. The accumulation of proline in *Prasiola crispa* during winter in Antarctica. *Physiologia Plantarum*, **94**, 25–30.

Jackson, A.E. & Seppelt, R.D. 1997. Physiological adaptations to freezing and UV radiation exposure in *Prasiola crispa*, an Antarctic terrestrial alga. *In* Battaglia, B., Valencia, J. & Walton, D.W.H., *eds.*, *Antarctic communities: species, structure, and survival*. Cambridge: Cambridge University Press, 226–233.

Kawahara, H. 2013. Characterizations of functions of biological materials having controlling-ability against ice crystal growth. *In* Ferreira, S.O., *ed.*, *Advance topics on crystal growth*. London: InTech, 119–143.

Kosugi, M., Katashima, Y., Aikawa, S., Tanabe, Y., Kudoh, S., Kashino, Y., *et al*. 2010. Comparative study on the photosynthetic properties of *Prasiola* (Chlorophyceae) and *Nostoc* (Cyanophyceae) from Antarctic and non-Antarctic sites. *Journal of Phycology*, **46**, 466–746.

Kovačik, L. & Pereira, A.B. 2001. Green alga *Prasiola crispa* and its lichenized form *Mastodia tesselata* in Antarctic environment: general aspects. *Nova Hedwigia. Beiheft*, **123**, 465–478.

Kovačik, L., Jancusova, M. & Pereira, A.B. 2003. Green alga *Prasiola crispa* (Lightf.) Menegh. and its lichenized form *Turgidosculum complicatulum* (Nyl.) J. Kohlm. & E. Kohlm. in Antarctic environment: variable of growth habit. *In* Olech, M.A., *ed., The functioning of polar ecosystems as viewed against global environmental changes.* Krakow: Institute of Botany, Jagiellonian University, 51–56.

Lud, D., Huiskes, A.H.L. & Ott, S. 2001a. Morphological evidence for the symbiotic character of *Turgidosculum complicatulum* Kohlm. & Kohlm. (= *Mastodia tesselata* Hook.f, & Harvey). *Symbiosis*, **31**, 141–151.

Lud, D., Buma, A.G.J., Van de Poll, W., Moerdijk, T.C.W. & Huiskes, A.H.L. 2001b. DNA damage and photosynthetic performance in the Antarctic terrestrial alga *Prasiola crispa* ssp. *antarctica* (Chlorophyta) under manipulated UV-B radiation. *Journal of Phycology*, **37**, 459–467.

Nowak, P., Harańczyk, H., Kijak, P., Fitas, J., Lisowska, M., Baran, E. & Olech, M.A. 2018. Bound water behavior in *Cetraria aculeata* thalli during freezing. *Polar Biology*, **41**, 865–876.

Pérez-Ortega, S., De Los Ríos, A., Crespo, A. & Sancho, L.G. 2010. Symbiotic lifestyle and phylogenetic relationships of the bionts of *Mastodia tesselata* (Ascomycota, *incertae sedis*). *American Journal of Botany*, **97**, 738–752.

Richter, D., Matuła, J., Urbaniak, J., Waleron, M. & Czerwik-Marcinowska, J. 2017. Molecular, morphological and ultrastructural characteristics of *Prasiola crispa* (Lightfoot) Kützing (Chlorophyta) from Spitsbergen (Arctic). *Polar Biology*, **40**, 379–397.

Santarius, K.A. 1992. Freezing of isolated thylakoid membranes in complex media. VIII. Differential cryoprotection by sucrose, proline and glycerol. *Physiologia Plantarum*, **84**, 87–93.

Storey, K.B. & Storey, J.M. 1996. Natural freezing survival in animals. *Annual Review of Ecology, Evolution, and Systematics*, **27**, 365–386.

Tatur, A., Myrcha, A. & Niegodzisz, J. 1997. Formation of abandoned penguin rookery ecosystems in the maritime Antarctica. *Polar Biology*, **17**, 405–417.

Valiullin, R. & Furo, I. 2002. The morphology of coexisting liquid and frozen phases in porous materials as revealed by exchange of nuclear spin magnetization followed by ^{1}H nuclear magnetic resonance. *Journal of Chemical Physics*, **117**, 2307–2316.

Wang, J., Xue, H., Zhou, B., Yao, Y.F. & Hansen, E.W. 2019. Interfacial water in mesopores and its implications to the surface features – a solid state NMR study. *Applied Surface Science*, **484**, 1154–1160.

Węglarz, W. & Harańczyk, H. 2000. Two-dimensional analysis of the nuclear relaxation function in the time domain: the program *CracSpin*. *Journal of Physics D: Applied Physics*, **33**, 1909–1920.

Wilson, P.W., Arthur, J.W. & Haymet, A.D.J. 1999. Ice premelting during differential scanning calorimetry. *Biophysical Journal*, **77**, 2850–2855.

Wilson, P.W., Heneghan, A.F. & Haymet, A.D.J. 2003. Ice nucleation in nature: supercooling point (SCP) measurements and the role of heterogeneous nucleation. *Cryobiology*, **46**, 88–98.

Wolfe, J., Bryant, G. & Koster, K.L. 2002. What is 'unfreezable water', how unfreezable is it, and how much is there? *CryoLetters*, **23**, 157–166.

Zhang, Z.Q., Liu, H.L., Liu, Z., Zhang, Z., Cheng, G.G., Wang, X.D. & Ding, J.N. 2019. Anisotropic interfacial properties between monolayered black phosphorus and water. *Applied Surface Science*, **475**, 857–862.

Zhou, J., Liu, Y., Zhou, X., Ren, J. & Zhong, C. 2018. Magnetic multi-porous bio-adsorbent modified with amino siloxane for fast removal of Pb(II) from aqueous solution. *Applied Surface Science*, **427**, 976–985.